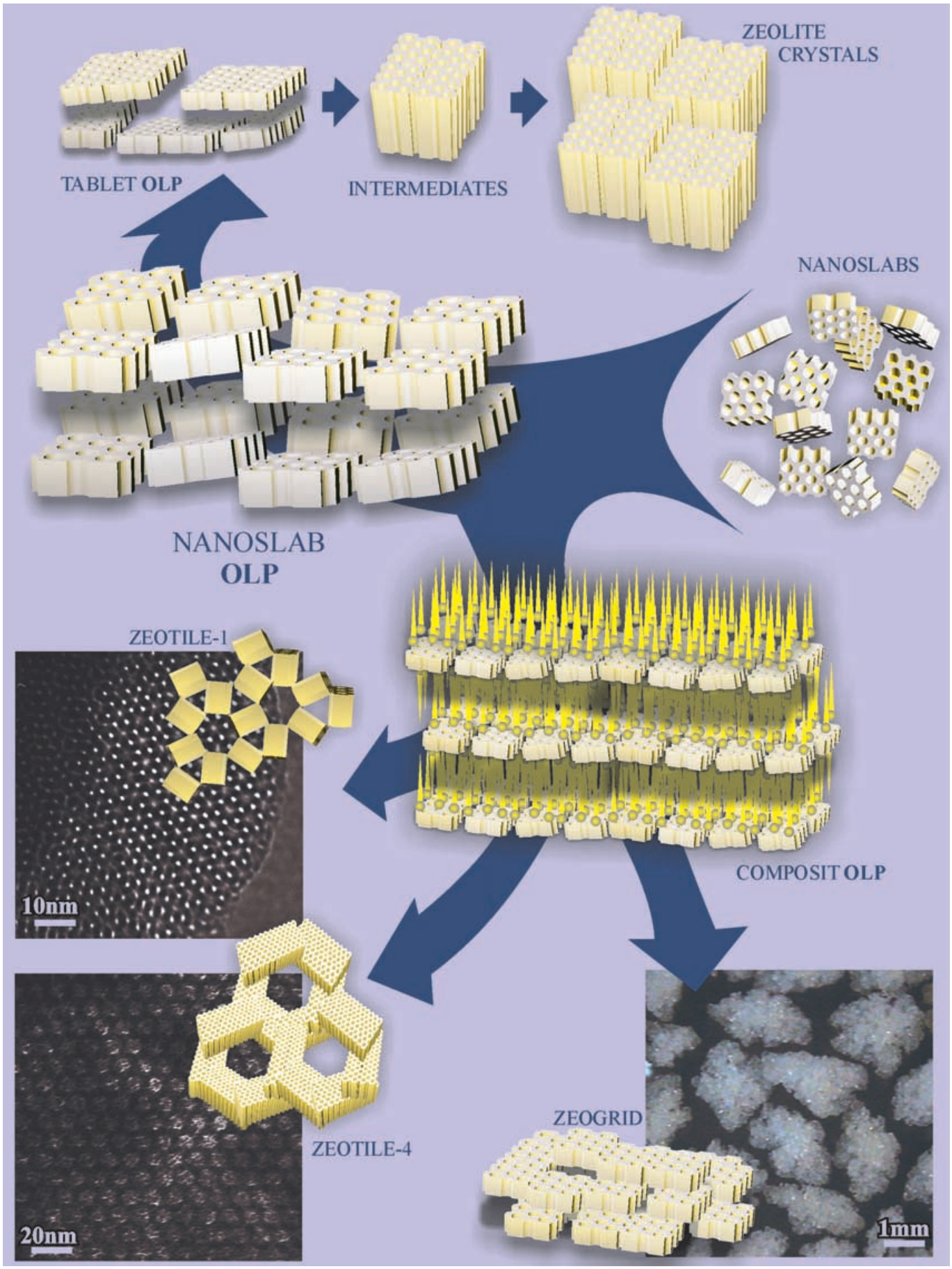

DOI: 10.1002/chem.200401329

Design and Synthesis of Hierarchical Materials from Ordered Zeolitic Building Units

Christine E. A. Kirschhock,[a] Sebastien P. B. Kremer,[a] Jan Vermant,[b] Gustaaf Van Tendeloo,[c] Pierre A. Jacobs,[a] and Johan A. Martens*[a]

Abstract: The crystallization of colloidal silicalite-1 from clear solution is one of the best understood zeolite formation processes. Colloidal silicalite-1 formation involves a self-assembly process in which nanoslabs and nanotablets with a silicalite-1 type connectivity are formed at intermediate stages. During the assembly process, with strongly anisometric particles present, regions appear with orientational correlations, as evidenced with measurements of dynamic light scattering, viscosity, and rotation of polarized light. The presence of such regions rationalizes the unexpected differences between the crystallization kinetics under microgravity and on earth. The discovery of the locally oriented regions sheds new light on currently poorly understood hydrodynamic effects on the zeolite formation processes, such as the influence of stirring on the phases obtained and the subsequent kinetics. Addition of surfactants or polymers modifies the ordering of the zeolitic building units in the correlated regions, and new types of hierarchical materials named zeogrids and zeotiles can be obtained.

Keywords: mesoporous materials · self-assembly · zeogrid · zeolites · zeotile

[a] Dr. C. E. A. Kirschhock, Dr. S. P. B. Kremer, Prof. P. A. Jacobs, Prof. J. A. Martens
Centre for Surface Chemistry and Catalysis, K.U. Leuven
Kasteelpark Arenberg 23, 3001 Leuven (Belgium)
Fax: (+32) 16-321-998
E-mail: johan.martens@agr.kuleuven.ac.be

[b] Prof. J. Vermant
Department of Chemical Engineering, K.U. Leuven
de Croylaan 46, 3001 Leuven (Belgium)

[c] Prof. G. Van Tendeloo
Centre for Electron Microscopy for Materials Science
University of Antwerp, Groenenborgerlaan 171
2020 Antwerpen (Belgium)

Introduction

Pores of inorganic materials are conventionally categorized into *micropores* with diameters smaller than 2 nm, *mesopores* with diameters from 2 to 50 nm, and *macropores* with diameters wider than 50 nm.[1] This IUPAC nomenclature is somewhat confusing, since the term micropores does not refer to micrometer dimension. The most popular microporous materials are the zeolites. Zeolites have a substantial impact on the economics and sustainability of products and processes in many sectors of industry.[2] Zeolite adsorbents and catalysts are the workhorses of petroleum refining operations and natural gas purification. Zeolites are used in large volumes as detergent builders and drying agents. Beside these classical uses, zeolite applications extend into a wealth of new areas including environmental protection, industrial production of fine chemicals that serve as, for example, pharmaceuticals, nutriceuticals, fragrances, flavors, and agrochemicals,[2] as well as sensors and electro-optical devices among other innovations.[3] After the development of zeolites, significant research efforts have been devoted to the synthesis of ordered mesoporous materials.[4] In contrast to zeolites, ordered mesoporous materials so far found little application, mainly because of the unspecific, amorphous nature of the walls separating the mesopores.[4]

A handicap of today's zeolite technology is the zeolite particle size of typically around one micrometer. There is a manifested interest in alternative structuring of zeolite matter, for example, to lift mass-transfer limitations of adsorption and catalysis in micrometer-sized zeolite crystals.[5] These shortcomings can, in principle, be overcome by generating mesopores in the zeolite crystals, as found in the ultrastabilization of zeolite Y, or development of nanozeolites,[6–9] or of zeolite films and membranes.[10,11] With respect to improved mass transfer, much is to be expected from hierarchical materials that have structural order at the meso- and/or macroscale in addition to the microscale. Structuring of zeolite crystallites at the macroscale has been achieved by using macroscopic templates.[12] Combined structuring at the

 DOI: 10.1002/chem.200401329

micro- and mesoscale is much less evident. The current approaches are presented schematically in Figure 1. Conventionally, a zeolite is crystallized by using molecular templates responsible for micropore formation. Noncrystalline mesoporosity in zeolite crystals can be obtained by hydro-

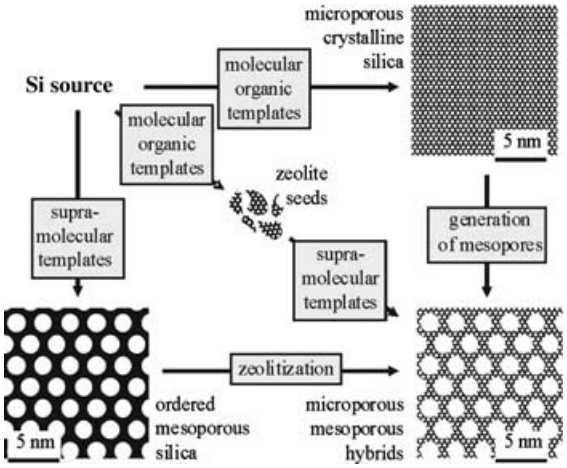

Figure 1. Strategies used to generate hierarchical materials.

thermal template syntheses within a mesoporous carbon matrix and subsequent combustion of the carbon.[13,14] Mesopores therein can be generated by controlled removal of the framework.[15] An alternative concept involves the synthesis of ordered mesoporous material with dense amorphous walls, followed by *zeolitization* of the walls under hydrothermal conditions.[16] A drawback of this last approach is that the formation of bulk zeolite and deterioration of the ordering at the meso scale are difficult to avoid. The reason for the slow progress in hierarchical material development is our limited understanding of the molecular mechanisms through which zeolite frameworks are actually assembled.[17,18]

The formation of a zeolite particle is a surprisingly slow process and strongly susceptible to stirring. Typically, a silicate-based hydrogel is converted into crystalline material through a lengthy hydrothermal treatment. Especially the syntheses of siliceous zeolites take from hours to days of processing time and require specific convective conditions. Why time and stirring have such an impact on the crystallization process is poorly understood at present. In our work we departed from the best understood zeolite synthesis, namely, that of silicalite-1, and demonstrate how this knowledge can be exploited in the development of hierarchical materials.

The Most Studied and Currently Best Understood Zeolite Synthesis: Silicalite-1

Since its discovery in 1978 as the first microporous crystalline silicon dioxide polymorph,[19] silicalite-1 has been the preferred study object of numerous studies dedicated to the formation process of a zeolite. The complexity of the formation process of this zeolite is reflected in the long time it took to unravel the molecular mechanism. A fair understanding of the molecular steps involved in the genesis of silicalite-1 crystals starting from silicate monomer was reached only recently for this unique case.[17,20] Key to this success was the use of a so-called "clear solution", which is a solution of tetrapropylammonium (TPA) silicate that is experimentally much more accessible than hydrogel systems. A transparent solution is obtained by reaction of tetraethylorthosilicate (TEOS) in aqueous tetrapropylammonium hydroxide. Silicalite-1 crystallizes from the clear solution upon heating according to the scheme presented in Figure 2.

Owing to its amphiphilic nature, TPA molecules are located at the interphase between the organic silicon phase and the aqueous phase. The TPA molecule takes charge of the silicate condensation steps from the beginning. Silicate polymerizes around the template into specific TPA–silicate entities, identified by spectroscopic methods.[21] The formation of specific open silicate molecules (Figure 2, species 1–4) during clear solution preparation was criticized.[22] Previously, only highly condensed, cagelike silicate species were observed in aqueous solutions. A comparison of the samples and their treatment from the earlier studies with the clear solutions revealed several differences. The open silicate species could only be detected in samples in which an interface between the hydrophobic silicon source and the aqueous template solution still existed. Furthermore, to prevent closure of the formed silicate species in an aqueous environment a very high TPA/silicon ratio is necessary. Also, any harsh sample treatments applied by other groups, like the boil–freeze–thaw cycle, results in destruction of the intermolecular template–silicate interactions.[23] Towards the end of the TEOS hydrolysis process, the hydrophobic–hydrophilic interface disappears and the cuplike silicate anions (species 3) need to rearrange to shield hydrophobic surfaces from the aqueous surrounding. This process culminates in the formation of the precursor (Figure 2, species 4). The precursor encapsulates one TPA ion and is already a specific fragment of the silicalite-1 structure. They offer an inner hydrophobic environment to the TPA molecule and a hydrophilic outer surface to the aqueous medium.

Through a combination of SAXS, AFM, dynamic light scattering (DLS), diffuse reflectance IR, and ^{29}Si NMR spectroscopy the aggregation steps starting from the precursor could be identified (Figure 2).[24] Precursors first link into rows of three (Figure 2, species 5), which click together sidewise into half-nanoslabs, nanoslabs ($4\times4\times1.3$ nm, species 7), and tablets ($8\times8\times1.3$ nm, species 8). This aggregation occurs usually at room temperature. The particle population that dominates in the final suspension depends on the TPA concentration, evaporation of ethanol, ionic strength, and the temperature. By careful adjustment of these parameters, suspensions of almost exclusively precursors, half-nanoslabs, nanoslabs, or tablets can be obtained (Figure 3).

Large efforts were invested in the attempt to capture nanoslabs on microscopic images (Figure 2, micrographs

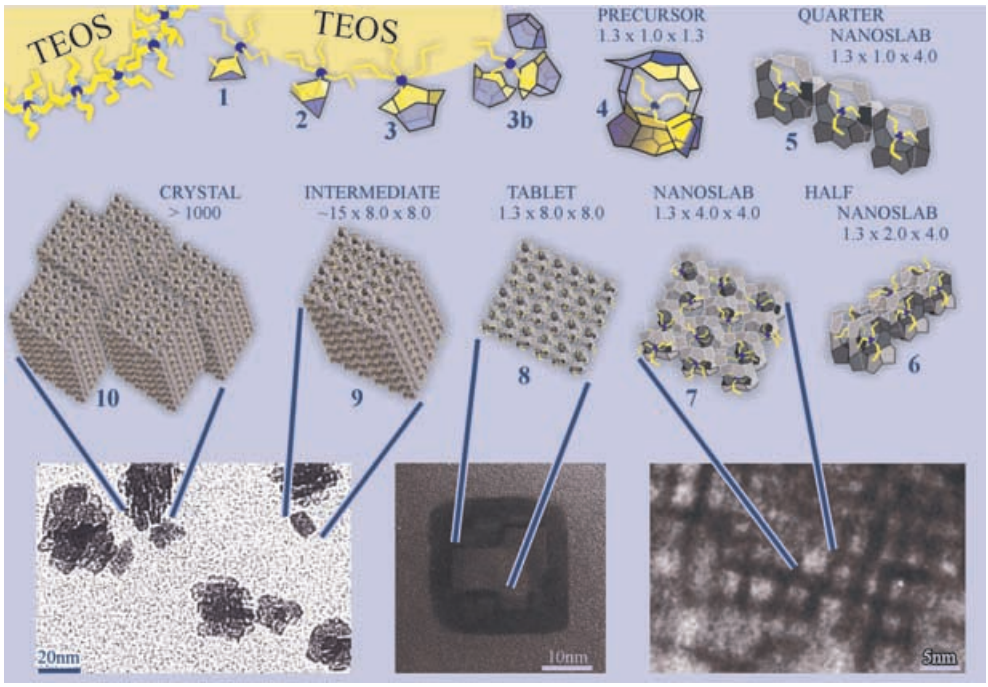

Figure 2. Formation of silicalite-1 type zeolite from clear solutions. Cryo-TEM picture (bottom left: courtesy of B. Schoeman).

center and right). A slight confusion arose after the original publication due to the presence of NaCl in the samples used for TEM studies.[25] It could be shown, however, that NaCl itself does not form entities of the observed shape and size. Instead, it was discovered that sodium cations closely interact with the negative charges on the anionic nanoslabs. It leads to the formation of a protective NaCl layer around the silicate entities during sample preparation that shields these fragile species from damage by the electron beam and allows recording of the morphology of the nanoslabs.[26]

Particle growth in a clear solution involves the approach and fusion of the entities shown in Figure 2 governed by colloid chemical principles. The general trend of particles to decrease their surface area is countered in this system by the surface charge and the presence of TPA cations in and around the negatively charged aggregating species. The electrostatic repulsion prevents undirected gelling. TPA cations within the precursor and adsorbed as a charge-compensating surface layer form a steric barrier with structure-directing properties. These barriers provoke the self-organizing process, resulting in larger and larger aggregates (Figure 2). After a colloidally stable particle distribution in the clear solution is reached, heating is required for the aggregation to proceed further. Stacking of the tablets into intermediates (Figure 2, species 9) occurs at elevated temperatures only. These intermediates finally fuse into silicalite-1 particles exhibiting crystallinity detected with XRD (species 10). The kinetic analysis of this self-organization within clear solutions upon heating confirmed the model of consecutive aggregation steps (Figure 4, top).

Occurrence of Complex Phase Behavior During the Colloidal Silicalite-1 Synthesis Process

Experimentation under microgravity conditions offers a unique means to assess the contribution of local particle interactions versus global convection in the ordering and aggregation of particles. Under microgravity, convective forces due to buoyancy and thermal density gradients are largely suppressed. The intriguing process of self-organization of small zeolitic building units into silicalite-1 (Figure 2) prompted the study of the transformation of fragments into silicalite-1 under microgravity conditions. During the ballistic rocket mission MAXUS 4, a 30 mini-autoclave unit with individually programmed heating and collective quenching was used to prepare series of quenched samples during silicalite-1 formation.[27] The evolution of the particle size populations was determined by using X-ray scattering in the transmission mode. It was found that microgravity conditions significantly slowed aggregation (Figure 4, bottom). Surprisingly, the aggregations of the smallest entities (fragments and nanoslabs) were most retarded under microgravity, namely, sixfold compared to 3.1- to 1.8-fold for intermediate and crystallite formation, respectively. Follow-up experiments aboard MAXUS 5 and the international space station confirmed this observation for different temperatures. The strongest retardation of the aggregation of the smallest particles was in apparent contradiction with the classical understanding. For the typical range of viscosity of the suspending medium, convection phenomena are expected to have an effect on micrometer-sized objects. The nano-

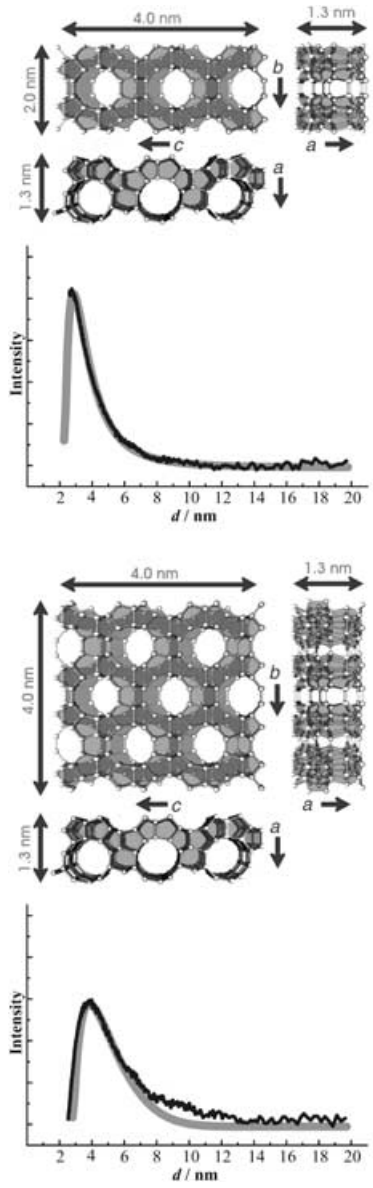

Figure 3. SAXS measurements of clear suspensions of half-nanoslabs (top) and nanoslabs (bottom). The measured data confirm the monomodal particle distribution and the presence of the illustrated particles (simulated scatter-curves in grey).

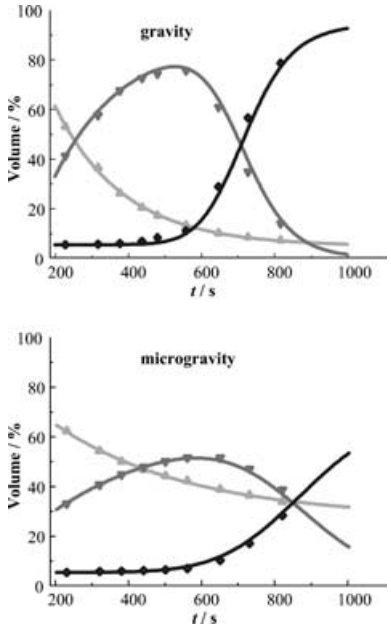

Figure 4. Population analysis of the formation of silicalite-1 from clear solutions at 155 °C. The experimental points were confirmed by kinetic simulations (curves). Light grey: small particles, nanoslabs, and tablets (Figure 2, species 5–8); dark grey: intermediates (species 9); black: crystals (species 10). Top: experiment under normal gravity; bottom: experiment under μg-conditions.

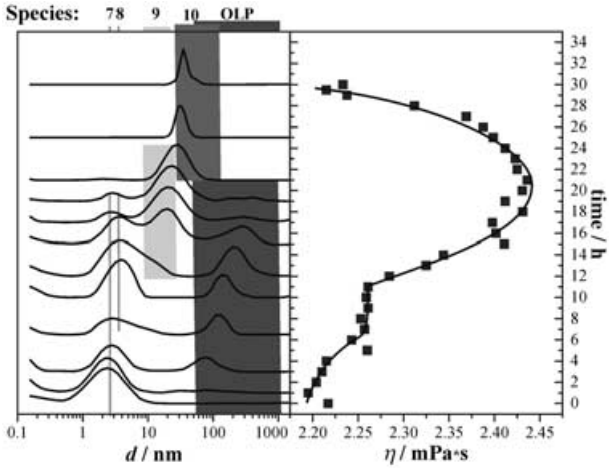

Figure 5. DLS (left) and viscosity (right) measurements of clear solutions during silicalite-1 formation at 80 °C. Tinted lines and bars indicate the presence of species 7 (nanoslabs), 8 (tablets), 9 (intermediates), and 10 (crystals; Figure 2), and OLPs, locally correlated regions.

meter-size regime should be completely governed by Brownian motion.

A first hint at an explanation for this unexpected microgravity effect was found during dynamic light scattering (DLS) investigations and viscosity measurements (Figure 5). Particle-size analysis, cross referenced with X-ray scattering, revealed the stepwise aggregation from fragments (d_{DLS} = 2.3 nm) to nanoslabs (d_{DLS} = 2.8 nm), tablets (d_{DLS} = 3.6 nm), intermediates (d_{DLS} = 20 nm), and final crystals (d_{DLS} = 35 nm) over the expected heating period. Surprisingly, parallel to these known aggregation steps, DLS revealed the existence of larger entities. A signal at approximately 75 nm that grew within the first hours, sharpened and shifted to about 200 nm after 12 h of heating. No particles of this size were present in clear solutions at these times according to X-ray scattering. Later, the unexpected DLS signal faded and finally disappeared. The occurrence of the DLS signal in the 75–200 nm range coincided with a temporary, 20 % increase of viscosity (Figure 5).

DLS gives insight into the mobility of the scattering particles. Interacting assemblies of particles appear as large entities, because their diffusion in the collective is strongly en-

cumbered. Consequently, the DLS signal above 75 nm is ascribed to fragments, nanoslabs, and tablets confined in locally correlated regions, which from now on we will call ordered liquid phases (OLPs). The particles involved are strongly negatively charged, are anisotropic and anisometric, and are covered with a layer of positively charged TPA cations. In addition, different populations of particle size and shape coexist during the synthesis process, making it hard to predict the phase behavior during the evolution of the synthesis process.

In general, local orientation correlation effects in a suspension are facilitated by the anisometry of the particle. Similar to the pretransitional effects in the case of liquid crystals, a strong sensitivity to flow effects can be expected, explaining the occurrence of the observed microgravity effects. Derjaguin, Landau, Verwey, Overbeek (DLVO) calculations on nanoslabs confirmed the existence of an energetic minimum for two particles at a distance of about 0.7 nm.[28] This energy minimum is consistent with a local stacking of the particles in the newly discovered OLPs.

These experiments revealed the important role of the large-scale orientation correlations that will be affected by the absence or presence of convection. The effects of flow on correlated regions rationalize the existence of a retardation effect of microgravity on the aggregation rate (Figure 4, bottom). Under microgravity, the effects of convective flows owing to buoyancy and density gradients are suppressed, and flow is known to affect the pretransitional phenomena.

The formation of the correlated domains was investigated in situ in the ZEOGRID hardware aboard the International Space Station.[29] The ZEOGRID hardware consists of 20 cartridges containing two fluids that can be manually mixed by turning a handle. One compartment contained TEOS, the other an aqueous solution of tetraproplyammoniumhydroxide (TPAOH), in proportions suitable for obtaining a nanoslab suspension under normal gravity conditions. Under microgravity conditions, millimeter-sized, solid particles were formed that clearly showed orientational order in small angle X-ray scattering measurements (Figure 6).

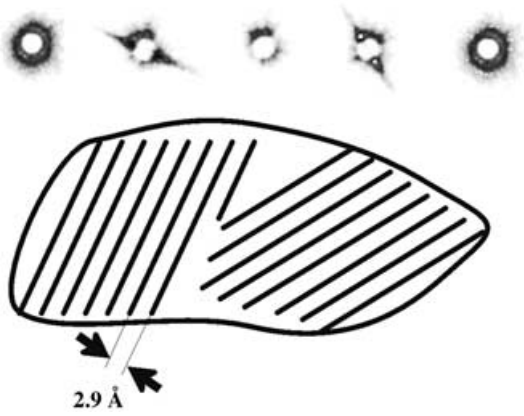

Figure 6. 2D SAXS measurement of solidified clear solution obtained under microgravity conditions. Analysis of intensity as a function of scattering angle revealed two layer-like domains of nanoslabs in the particle.

Closer analysis revealed these particles to consist of nanoslabs that were embedded layer-wise into a matrix of TPA cations with a repetitive *d* value of 29 A. This experiment provided strong evidence for the favored self-organization of nanoslabs into ordered phases under microgravity conditions.

Manipulation of Ordered Domains to Obtain Self-Assembly into Hierarchical Materials

The discovery of correlated "domains" and its influence on the kinetics as an explanation for the unexpected microgravity effects certainly is very attractive from a scientific point of view. Furthermore, the improved understanding of the self-organization of zeolitic building units in OLPs had significant impact on the development of new application-oriented materials. Through mastering of the formation of orientational order, design of zeolites on demand appears to be within reach. Already now, with only vague understanding of the interparticle interactions leading to the ordering and the structure of the "domains", two new types of hierarchical materials could be developed by modifying the ordering of the building units through addition of surfactants and polymers (Figure 7).

The first type of material, denoted as zeogrid,[30] was obtained by reorganization of the correlated regions by addition of cetyltrimethylammonium bromide (CTAB). The nanoslabs are stacked in concentric layers, intercalated by surfactant molecules. Removal of the surfactant through calcination causes partial fusion of the nanoslabs. Empty spaces left laterally between individual nanoslabs are responsible for super-microporosity and provide access to the zeolite pores provided by the nanoslabs.

In the second type of hierarchical structure, denoted as zeotiles (Figure 7), nanoslabs are linked through their corners, edges, or faces following patterns imposed by interaction with surfactant or triblock copolymer.[31] A remarkably high mesostructural order is typical for these assemblies. After evacuation of the organics, microporosity inside the nanoslabs and an exceptionally open mesopore network between the nanoslabs, depending on the tiling pattern of the slabs, is obtained.

The morphology and structure of zeogrids and zeotiles was observed to be highly sensitive to the mixing conditions, suggesting a strong impact of convection on the nanoslab ordering process upon surfactant addition. To clarify this effect, a series of 20 different zeogrid syntheses was performed in the above-mentioned ZEOGRID hardware aboard the International Space Station. Nanoslab suspensions were mixed with the surfactant solutions in space. Throughout, it was observed that the samples obtained under microgravity conditions were of larger size, monolithic character, and better ordered internally (Figures 7 and 8). These observations indicate that shear flow and convection effects have a major role in arranging the elementary building units before solidification occurs. A closer analysis of

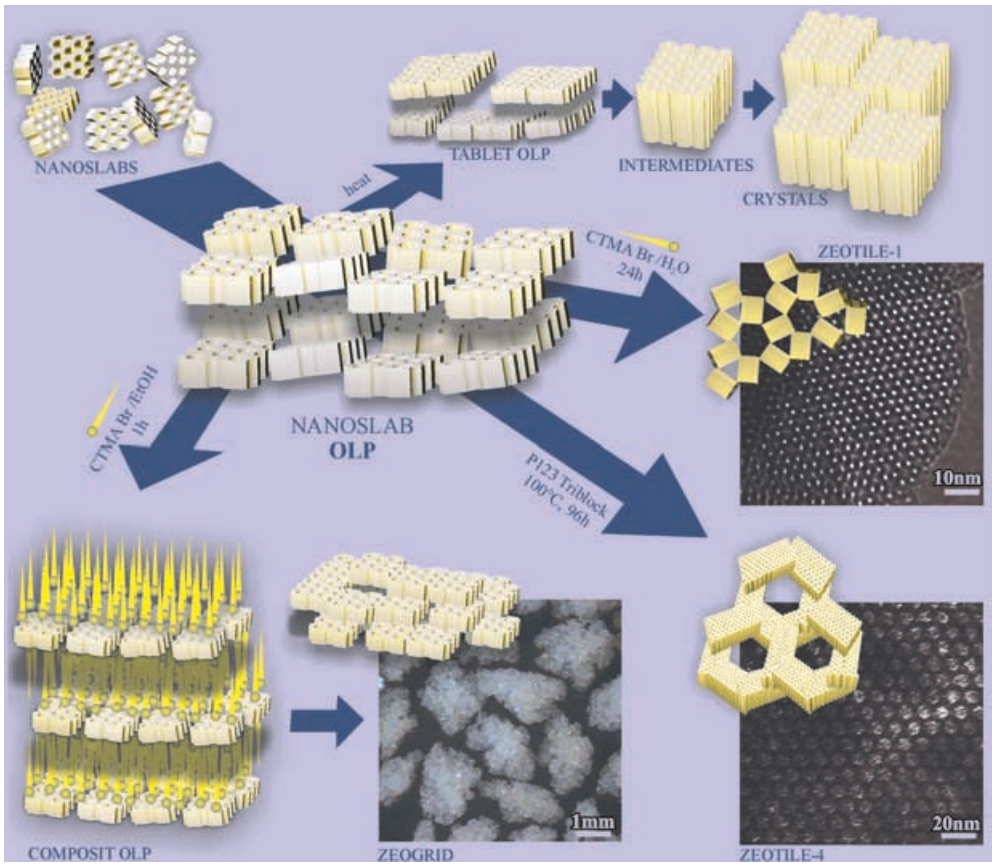

Figure 7. Manipulation of nanoslab OLPs results in different materials.

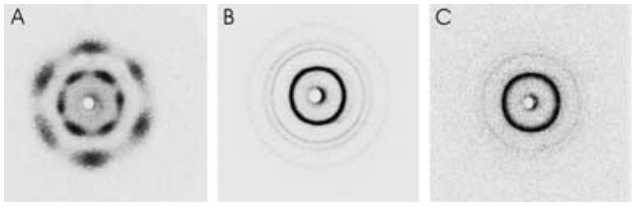

Figure 8. 2D SAXS measurement of zeotile-1. A) Monolithic mm-sized particle obtained under μg-conditions; B) same sample as in A, but powdered; C) sample obtained under 1 g, no big particles were obtained.

the rules governing the complex phase behavior will certainly lead to new synthesis strategies to modify the aggregation product from within those phases in a directed manner.

Conclusions and Perspectives

The study case of formation and ordering of regular silicalite building units shows that understanding of the molecular and supermolecular template effect leads towards expertise in design of application-oriented materials. Even though the existence of nanoslabs and their organization into orientationally correlated domains is observed only for silicalite-1 and -2 zeolites, there are some indications that this is not an isolated occurrence. For mesoporous materials, the occurrence of ordered surfactant–silicate lamellar phases with unstructured silica species has been observed before.[32–33] Also, the self-assembly of larger colloidal Bragg crystalline particles has been observed and studied.[12] The concept of using prefabricated zeolite nuclei in the synthesis of mesoporous materials[34–41] also entirely depends on the existence of structured zeolite building units, the self-assembly of which is certainly ruled by similar colloidal interactions as the herein described aggregation of nanoslabs within orientationally correlated domains. Another hint for the existence of ordering is the common observation in several template-directed zeolite syntheses of the formation of layered precursor structures.[42–46] The discovery of the orientationally correlated domains offers a new concept for rationalizing the phenomena during the genesis of micro- and mesoporous materials from elemental building units.

Acknowledgements

C.E.A.K., S.P.B.K., P.A.J., and J.A.M. thank the Belgian Government for supporting an Interuniversity Pole of Attraction (IPA-PAI). ESA and the Prodex office are acknowledged for financing of the microgravity experiments. C.E.A.K. acknowledges the FWO for a funding of a postdoctoral position. We thank Liesbeth Theunissen for her work on the viscosity measurements.

[1] J. Rouquerol, D. Avnir, C. W. Fairbridge, D. H. Everett, J. H. Haynes, N. Pernicone, J. D. F. Ramsay, K. S. W. Sing, K. K. Unger, *Pure Appl. Chem.* **1994**, *66*, 1739–1758.
[2] *Zeolites for Cleaner Technologies* (Eds.: M. Guisnet, J.-P. Gilson), Imperial College Press, London, UK, **2002**.
[3] M. E. Davis, *Nature* **2002**, *417*, 813–821.
[4] M. Antonietti, G. A. Ozin, *Chem. Eur. J.* **2004**, *10*, 29–41.
[5] J. A. Martens, P. A. Jacobs, *Adv. Funct. Mater.* **2001**, *11*, 337–338.
[6] B. J. Schoeman, J. Sterte, J. E. Otterstedt, *J. Chem. Soc. Chem. Commun.* **1993**, 994–995.
[7] S. Mintova, N. H. Olson, V. Valtchev, T. Bein, *Science* **1999**, *283*, 958–960.
[8] Y. Tao, H. Kanoh, K. Kaneko, *J. Am. Chem. Soc.* **2003**, *125*, 6044–6045.
[9] I. Schmidt, C. Madsen, C. J. H. Jacobsen, *Inorg. Chem.* **2000**, *39*, 2279–2283.
[10] K. Jansen, T. Maschmeyer, *Top. Catal.* **1999**, *9*, 113–122.
[11] M. Tsapatsis, D. G. Vlachos, *Science* **2003**, *300*, 456–460.
[12] V. Valtchev, *Chem. Mater.* **2002**, *14*, 4371–4377.
[13] C. J. H. Jacobsen, C. Madsen, J. Houzvicka, I. Schmidt, A. Carlsson, *J. Am. Chem. Soc.* **2000**, *122*, 7116–7117.
[14] M. Hartmann, *Angew. Chem.* **2004**, *16*, 6004–6006; *Angew. Chem. Int. Ed.* **2004**, *43*, 5880–5882.
[15] D. Khushalani, A. Kuperman, G. A. Ozin, K. Tanaka, J. Garces, M. M. Olken, N. Coombs, *Adv. Mater.* **1995**, *7*, 842–846.
[16] D. T. On, D. Lutic, S. Kaliaguine, *Microporous Mesoporous Mater.* **2001**, *44*, 435–444.
[17] C. S. Cundy, P. A. Cox, *Chem. Rev.* **2003**, *103*, 663–701.
[18] G. J. A. A. Soler-Illia, C. Sanchez, B. Lebeau, J. Patarin, *Chem. Rev.* **2002**, *102*, 4093–4138.
[19] E. M. Flanigen, J. M. Bennett, R. W. Grose, J. P. Cohen, R. L. Patton, R. M. Kirschner, J. V. Smith, *Nature* **1978**, *271*, 512–516.
[20] C. E. A. Kirschhock, V. Buschmann, S. Kremer, R. Ravishankar, C. J.Y Houssin, B. L. Mojet, R. A. van Santen, P. J. Grobet, P. A. Jacobs, J. A. Martens, *Angew. Chem.* **2001**, *113*, 2707–2710; *Angew. Chem. Int. Ed.* **2001**, *40*, 2637–2640.
[21] C. E. A. Kirschhock, R. Ravishankar, F. Verspeurt, P. J. Grobet, P. A. Jacobs, J. A. Martens, *J. Phys. Chem. B* **1999**, *103*, 4965–4971.
[22] C. T. G. Knight, S. D. Kinrade, *J. Phys. Chem. B* **2002**, *106*, 3329–3332.
[23] C. E. A. Kirschhock, R. Ravishankar, F. Verspeurt, P. J. Grobet, P. A. Jacobs, J. A. Martens, *J. Phys. Chem. B* **2002**, *106*, 3333–3334.
[24] C. E. A. Kirschhock, R. Ravishankar, L. Van Looveren, P. A. Jacobs, J. A. Martens, *J. Phys. Chem. B* **1999**, *103*, 4972–4978.
[25] H. Ramanan, E. Kokkoli, M. Tsapatsis, *Angew. Chem.* **2004**, *116*, 4658–4661; *Angew. Chem. Int. Ed.* **2004**, *43*, 4558–4561.
[26] C. E. A. Kirschhock, D. Liang, A. Aerts, C. A. Aerts, S. P. B. Kremer, P. A. Jacobs, G. Van Tendeloo, J. A. Martens, *Angew. Chem.* **2004**, *116*, 4662–4664; *Angew. Chem. Int. Ed.* **2004**, *43*, 4562–4564.
[27] S. P. B. Kremer, E. Theunissen, C. E. A. Kirschhock, J. A. Martens, P. A. Jacobs, W. Herfs, *Adv. Space Res.* **2003**, *32*, 259–263.
[28] C. E. A. Kirschhock, R. Ravishankar, P. A. Jacobs, J. A. Martens, *J. Phys. Chem. B* **1999**, *103*, 11021–11027.
[29] S. Kremer, C. Kirschhock, J. A. Martens, P. A. Jacobs, V. Pletser, O. Minster, R. Kassel, in *Proc. Int. Zeolite Conf. 14th*, in press.
[30] S. P. B. Kremer, C. E. A. Kirschhock, M. Tielen, F. Collignon, P. J. Grobet, P. A. Jacobs, J. A. Martens, *Adv. Funct. Mater.* **2002**, *12*, 286–292.
[31] S. P. B. Kremer, C. E. A. Kirschhock, A. Aerts, K. Villani, J. A. Martens, O. I. Lebedev, G. Van Tendeloo, *Adv. Mater.* **2003**, *15*, 1705–1707.
[32] S. C. Christiansen, D. Y. Zhao, M. T. Janicke, C. C. Landry, G. D. Stucky, B. F. Chmelka, *J. Am. Chem. Soc.* **2001**, *123*, 4519–4529.
[33] C. C. Landry, S. H. Tolbert, K. W. Gallis, A. Monnier, G. D. Stucky, P. Norby, J. C. Hanson, *Chem. Mater.* **2001**, *13*, 1600–1608.
[34] R. W. Hicks, T. J. Pinnavaia, *Chem. Mater.* **2003**, *15*, 78–82.
[35] Y. Han, S. Wu, Y. Sun, D. Li, F.-S. Xiao, *Chem. Mater.* **2002**, *14*, 1144–1148.
[36] J. Liu, X. Zhang, Y. Han, F.-S. Xiao, *Chem. Mater.* **2002**, *14*, 2536–2540.
[37] S. P. Naik, A. S. T. Chiang, R. W. Thompson, F. C. Huang, H.-M. Kao, *Microporous Mesoporous Mater.* **2003**, *60*, 213–224.
[38] P. Prokesova, S. Mintova, J. Cejka, T. Bein, *Microporous Mesoporous Mater.* **2003**, *64*, 165–174.
[39] C. S. Carr, S. Kaskel, D. F. Shantz, *Chem. Mater.* **2004**, *16*, 3139–3146.
[40] L. M. Huang, Z. B. Wang, J. Y. Sun, L. Miao, Q. Z. Li, Y. S. Yan, D. Y. Zhao, *J. Am. Chem. Soc.* **2000**, *122*, 3530–3531.
[41] N. Hedin, R. Graf, S. C. Christiansen, C. Gervais, R. C. Hayward, J. Eckert, B. F. Chmelka, *J. Am. Chem. Soc.* **2004**, *126*, 9425–9432.
[42] H. van Koningsveld, H. Gies, *Z. Kristallogr.* **2004**, *219*, 637–643.
[43] A. Corma, V. Fornes, J. M. Guil, S. B. Pergher, Th. L. M. Maesen, J. G. Buglass, *Microporous Mesoporous Mater.* **2000**, *38*, 301–309.
[44] Y. Zhou, M. Antonietti, *Chem. Mater.* **2004**, *16*, 544–550.
[45] F. Taulelle, M. Pruski, J. P. Amoureux, D. Lang, A. Bailly, C. Huguenard, M. Haouas, C. Gerardin, T. Loiseau, G. Ferey, *J. Am. Chem. Soc.* **1999**, *121*, 12148–12153.
[46] L. Schreyeck, P. Caullet, J. C. Mougenel, B. Marler, *Microporous materials* **1996**, *6*, 259–271.

Published online: May 4, 2005

